High penetration of ultraviolet radiation in the south east Pacific waters

Marc Tedetti,[1] Richard Sempéré,[1] Alexander Vasilkov,[2] Bruno Charrière,[1] David Nérini,[1] William L. Miller,[3] Kimitaka Kawamura,[4] and Patrick Raimbault[5]

Received 27 February 2007; revised 26 April 2007; accepted 16 May 2007; published 27 June 2007.

[1] We investigated the penetration of solar ultraviolet radiation (UVR) in the surface waters of the south east Pacific (08–35°S, 142–73°W) from October to December 2004 during the BIOSOPE cruise. In the hyper-oligotrophic waters of the South Pacific Gyre (near Easter Island), diffuse attenuation coefficients for downward irradiance, $K_d(\lambda)$, at 305 nm (UV-B), 325, 340 and 380 nm (UV-A) were 0.083, 0.055, 0.039 and 0.021 m^{-1}, respectively. The corresponding 10% irradiance depths, $Z_{10\%}(\lambda)$, were 28, 42, 59 and 110 m, respectively. These UVR penetrations are the highest ever reported for oceanic waters and are equal to those measured in the clearest fresh waters. UV-extended inherent optical property (IOP) and radiative transfer (RT) models allowed reliable estimations of $K_d(\lambda)$ with the Case 1 water assumption when two values of chromophoric dissolved organic matter (CDOM) absorption spectral slope coefficient (S) were used, i.e. 0.017 nm^{-1} at 325, 340 and 380 nm, and 0.023 nm^{-1} at 305 nm. **Citation:** Tedetti, M., R. Sempéré, A. Vasilkov, B. Charrière, D. Nérini, W. L. Miller, K. Kawamura, and P. Raimbault (2007), High penetration of ultraviolet radiation in the south east Pacific waters, *Geophys. Res. Lett.*, *34*, L12610, doi:10.1029/2007GL029823.

1. Introduction

[2] The current context of stratospheric ozone depletion and climate change has fueled interest in studying the impact of solar ultraviolet radiation (UVR) on marine ecosystems [*Whitehead et al.*, 2000]. In the surface ocean, both UV-B (280–315 nm) and UV-A (315–400 nm) induce photo-degradation of chromophoric dissolved organic matter (CDOM) [*Mopper and Kieber*, 2002] and photo-production of DNA damages in bacterio- and phyto-plankton [*Buma et al.*, 2003]. Therefore, accurate measurements of underwater UV-B and UV-A irradiances are essential in assessing the quantitative effect of UVR on the marine carbon cycle.

[3] UVR measurements have been reported in various oceanic environments such as open oceans, Antarctic waters and coastal areas (see review by *Tedetti and Sempéré* [2006]). However, only *Morel et al.* [2007] reported such measurements in the south east Pacific, and especially in the anticyclonic South Pacific Gyre (SPG), which remains one of the less studied major oceanic regimes. According to ocean color data, the center of the SPG (near Easter Island) has very low chlorophyll a (Chl a) concentrations in the surface waters (below 0.03 mg m^{-3}) [*Fougnié et al.*, 2002; *Claustre and Maritorena*, 2003]. These waters, too far from any continents to receive nutritive elements via rivers or aerosols, are characterized as ''hyper-oligotrophic'' [*Claustre and Maritorena*, 2003].

[4] Recently, *Vasilkov et al.* [2001] have provided global mapping of UVR penetrations into the ocean waters. They combined the Total Ozone Monitoring Spectrometer (TOMS) satellite estimates of surface UV irradiance with the Sea-viewing Wide Field-of-view Sensor (SeaWiFS) satellite estimates of surface Chl a, and used inherent optical property (IOP) and oceanic radiative transfer (RT) models extrapolated to the UV spectral domain.

[5] The main objectives of the present study are **(i)** To assess from in situ optical measurements, the penetration of UV-B and UV-A irradiances in the surface waters of the south east Pacific including the hyper-oligotrophe zone of the SPG and **(ii)** To compare these in situ UVR penetrations with the UVR penetrations computed from IOP and RT models.

2. Experimental

[6] In situ measurements were performed at thirteen stations along a 8000-km transect from the mesotrophic waters near Marquesas Islands (08°S, 142°W) through the hyper-oligotrophic waters of the SPG (vicinity of Easter Island: 20–30°S, 98–122°W) to the coastal eutrophic waters associated to upwelling off Chile (35°S, 73°W) during the Biogeochemistry and Optics South Pacific Experiment (BIOSOPE) cruise (October–December 2004) (Figure 1).

[7] Two profiles of downward irradiance ($E_d(Z, \lambda)$ in $\mu W\ cm^{-2}\ nm^{-1}$) and upward radiance ($L_u(Z, \lambda)$ in $\mu W\ cm^{-2}\ nm^{-1}\ sr^{-1}$) were made at each station (Figure 1) around solar noon using a Satlantic MicroPro free-fall profiler equipped with OCR-504 downward irradiance and upward radiance sensors in the UV-B (305 nm), UV-A (325, 340 and 380 nm) and visible (412, 443, 490 and 565 nm) spectral domains. Surface irradiance ($E_s(\lambda)$ in $\mu W\ cm^{-2}\ nm^{-1}$), which is equivalent to the downward irradiance just above the sea surface ($E_d(0^+, \lambda)$), was simultaneously

[1]Laboratoire de Microbiologie Géochimie et Ecologie Marines (LMGEM), UMR 6117, Centre d'Océanologie de Marseille, Université de la Méditerranée, Campus de Luminy, Marseille, France.
[2]Science Systems and Applications, Inc., Lanham, Maryland, USA.
[3]Department of Marine Sciences, University of Georgia, Athens, Georgia, USA.
[4]Institute of Low Temperature Science, Hokkaido University, Sapporo, Japan.
[5]Laboratoire d'Océanographie et de Biogéochimie, UMR 6535, Centre d'Océanologie de Marseille, Université de la Méditerranée, Campus de Luminy, Marseille, France.

0094-8276/07/2007GL029823$05.00

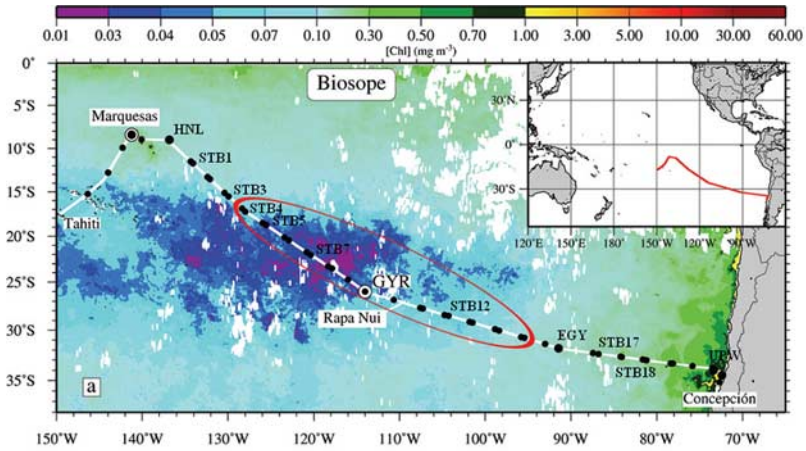

Figure 1. Map of the BIOSOPE cruise track superimposed on a MERIS composite image (level 3) for August 2004, showing the chlorophyll concentration in the upper layer. The stations include Marquesas Islands (MAR), high nutrients low chlorophyll zone (HNL), center of South Pacific Gyre (GYR), East of South Pacific Gyre (EGY) and upwelling off Chile (UPW). The stations exhibiting the clearest waters are inside the red ellipse. Rapa Nui is Easter Island. Copyright (2007) by the American Society of Limnology and Oceanography, Inc. [*Morel et al.*, 2007, p. 219].

measured at the same channels on the ship deck using other OCR-504 sensors to account for the variations of cloud conditions during the cast. For in-water sensors, the Full-Width Half-Maximum (FWHM) of the channels was 2 nm for 305, 325 and 340 nm, and 10 nm for 380, 412, 443, 490 and 565 nm. For in-air sensors, the FWHM of the channels was 2 nm for 305, 325 and 340 nm, 10 nm for 380 nm, and 20 nm for 412, 443, 490 and 565 nm. The MicroPro free-fall profiler was operated from the rear of the ship and deployed 20–30 m away to minimize the shadowing effects and disturbances of the ship.

[8] Profiles of downward irradiance in the spectral range of photosynthetically available radiation (PAR: 400–700 nm) were estimated from the four visible channels using Satlantic's Prosoft software. $E_d(\lambda)$ was first interpolated onto an 1 nm interval from 400 to 700 nm and then integrated using the formula:

$$E_{d,PAR}(Z) = \int_{400\ nm}^{700\ nm} \lambda/hc\, E_d(Z,\lambda)d\lambda \quad (1)$$

where $E_{d,PAR}(Z)$ is the downward irradiance in the spectral range of PAR at depth Z (quanta cm^{-2} s^{-1}), λ is the wavelength (nm), h is the Planck's constant ($6.63.10^{-34}$ J s), c is the speed of light in the vacuum (3.10^8 m s^{-1}) and $E_d(Z, \lambda)$ is the downward irradiance at depth Z (μW cm^{-2} nm^{-1}). Diffuse attenuation coefficients for downward UV and PAR irradiances ($K_d(\lambda)$ and $K_{d,PAR}$ in m^{-1}) were calculated for the depth interval 0^- to Z (m), i.e. 6, 15 or 30 m from the slope of the linear regression of the log-transformed downward irradiance versus depth in accordance with the relationship:

$$E_d(Z,\lambda) = E_d(0^-,\lambda)\exp[-K_d(\lambda)Z] \quad (2)$$

where $E_d(0^-, \lambda)$ is the downward irradiance beneath the surface. Because of the wave-focusing effects leading to fluctuations in in-water irradiance near the surface, irradiance data of the first meters were omitted from the calculation and $E_d(0^-, \lambda)$ was theoretically computed from deck measurements using the formula [*Smith and Baker*, 1984]:

$$E_d(0^-,\lambda) = E_s(\lambda)/(1+\alpha) \quad (3)$$

where α (0.043) is the Fresnel reflection albedo for irradiance from sun and sky. The 10% irradiance depth ($Z_{10\%}(\lambda)$ in m), which is the depth where the downward irradiance is 10% of its surface value, was determined from $K_d(\lambda)$:

$$Z_{10\%}(\lambda) = \ln(10)/K_d(\lambda) = 2.30/K_d(\lambda) \quad (4)$$

[9] Seawater samples for discrete Chl a analysis were taken at each station, except UPW (Figure 1), at 5–20 m depth using 12-L Niskin bottles. Chl a concentration was determined by using fluorescence technique [*Herbland et al.*, 1985]. In UPW, surface Chl a was estimated from $L_u(Z, \lambda)$ and $E_s(\lambda)$ measurements by using the bio-optical equations by *Gordon et al.* [1988] validated in previous SeaWiFS observations. Primary production (PP) was evaluated in MAR, SPG and UPW with the dual isotopic $^{15}N/^{13}C$ method [*Raimbault et al.*, 1999].

[10] $K_d(\lambda)$ was also computed from UV-extended IOP and RT models according to *Vasilkov et al.* [2005]. Briefly, the UV-extended IOP model is a standard three-parameter (Chl a concentration, CDOM absorption and particulate matter scattering) model that can be reduced to either the one-parameter Case 1 water model or two-parameter model. In the Case 1 water model, the only input parameter is Chl a concentration since CDOM absorption at 440 nm is assumed to be 20% of the total absorption of pure seawater and phytoplankton [*Morel*, 1988; *Morel and Maritorena*, 2001]:

$$a_{CDOM}(440) = 0.2\left[a_w(440) + a_{ph}(440)\right] \quad (5)$$

Table 1. Station Location, Date of Measurement, Deep Chlorophyll Maximum, in Situ Surface Chl a Concentration, and Diffuse Attenuation Coefficients for UV-B, UV-A, and PAR Downward Irradiance[a]

					$K_d(\lambda)$, m^{-1}				
Station	Position	Date	DCM, m	Chl a, mg m^{-3}	305 nm	325 nm	340 nm	380 nm	$K_{d,PAR}$
MAR	08°S, 142°W	29 Oct. 04	60	0.320	0.239	0.134	0.099	0.062	0.058
HNL	09°S, 137°W	2 Nov. 04	80	0.152	0.228	0.110	0.079	0.049	0.055
STB1	12°S, 134°W	3 Nov. 04	80	0.172	0.192	0.107	0.078	0.041	0.048
STB3	16°S, 130°W	5 Nov. 04	120	0.061	0.190	0.085	0.061	0.037	0.040
STB4	17°S, 128°W	6 Nov. 04	130	0.060	0.139	0.066	0.048	0.025	0.033
STB5	19°S, 126°W	7 Nov. 04	140	0.049	0.121	0.061	0.043	0.024	0.028
STB7	22°S, 120°W	9 Nov. 04	195	0.027	0.083	0.055	0.039	0.024	0.027
GYR	26°S, 114°W	15 Nov. 04	180	0.029	0.108	0.057	0.040	0.021	0.025
STB12	29°S, 104°W	21 Nov. 04	180	0.029	0.122	0.058	0.041	0.024	0.025
EGY	32°S, 91°W	28 Nov. 04	80	0.084	0.194	0.101	0.081	0.043	0.050
STB17	32°S, 87°W	1 Dec. 04	70	0.132	0.234	0.125	0.094	0.052	0.052
STB18	33°S, 84°W	2 Dec. 04	70	0.139	0.259	0.143	0.104	0.059	0.057
UPW	34°S, 73°W	6 Dec. 04	40	1.442[b]	0.756	0.466	0.394	0.261	0.144

[a]UV-B is 305 nm; UV-A is 325, 340, and 380 nm; PAR is 400–700 nm; DCM denotes deep chlorophyll maximum; Diffuse attenuation coefficients for UV and PAR downward irradiance are Kd(λ) and Kd, PAR. Averaged $K_d(\lambda)$ and $K_{d,PAR}$ presented here are based on two downward irradiance profiles (CV < 5%). $K_d(\lambda)$ and $K_{d,PAR}$ were determined over the depth interval 0^- to 6, 15 or 30 m and the determination coefficients (r^2) of their calculations were >0.97 for all the stations. Averaged in situ surface Chl a concentrations presented here are based on duplicate analyses (CV < 8%).
[b]Surface Chl a was estimated from $L_u(Z, \lambda)$ and $E_s(\lambda)$ measurements by using the bio-optical equations by *Gordon et al.* [1988].

where a_{CDOM}, $a_w(440)$ and $a_{ph}(440)$ are absorption coefficient of CDOM, pure seawater and phytoplankton at 440 nm, respectively. The two-parameter model assumes two input independent parameters including Chl a concentration and CDOM absorption at a reference wavelength. In both cases, pure seawater absorption is interpolated between experimental data sets available in the literature as recommended by *Fry* [2000].

[11] In this study, since in situ CDOM absorption data were not available, the UV-extended IOP model was used with in situ surface Chl a concentration as input parameter assuming the Case 1 water model. We adopted an average value of CDOM absorption spectral slope coefficient over the UV domain S = 0.017 nm^{-1} as proposed by *Kopelevich et al.* [1989]. CDOM absorption at a given wavelength over the UV spectral domain, $a_{CDOM}(\lambda)$, was then derived from S and $a_{CDOM}(440)$ according to the formula:

$$a_{CDOM}(\lambda) = a_{CDOM}(440)\exp[-S(\lambda - 440)] \quad (6)$$

The in-water lookup tables for downward irradiances were pre-computed with the full RT model Hydrolight [*Mobley*, 1994] for vertically homogeneous waters, Chl a concentrations ranging from 0.01 to 5 mg m^{-3}, CDOM absorption coefficients at 400 nm ranging from 0 to 0.3 m^{-1} and solar zenith angle (SZA) ranging from 0 to 80°. The surface lookup tables were generated for clear skies and cloudy conditions (cloud fraction from 0 to 100%) with ozone amounts ranging from 125 to 575 Dobson Unit.

3. Results and Discussion

[12] In situ surface Chl a, in accordance with ocean color observations, showed considerable variations across the south east Pacific. In the center of the SPG (STB7, GYR and STB12), surface Chl a was minimal, with concentrations lower than 0.03 mg m^{-3}, even though a deep chlorophyll maximum (DCM) was detected as deep as 180 to 195 m (Table 1). In this area, PP was strongly nutrient-limited (PP integrated within surface and euphotic zone, I-PP: 159–206 mg C m^{-2} d^{-1}) with regard to the absence of terrestrial inputs and the depth of nutricline (1 μM N at ~200 m). By contrast, in the Marquesas Islands (MAR), surface Chl a (0.320 mg m^{-3}; Table 1) was higher than that generally observed (~0.1 mg m^{-3}) in this high nutrients low chlorophyll (HNLC) subequatorial area at other periods of the year [*Signorini et al.*, 1999], very likely in relation with coastal hydrodynamic structures favoring the input of iron from islands into surrounding waters [*Andrié et al.*, 1992] and subsequent phytoplankton growths (I-PP: 537–720 mg C m^{-2} d^{-1}). In the upwelling off Chile (UPW), surface Chl a and I-PP were much higher than those measured in MAR with 1.4 mg m^{-3} (Table 1) and 3784 mg C m^{-2} d^{-1}, respectively. From October to March, wind-driven coastal upwelling fertilizes the surface waters off Chile which leads to one of the most productive areas in the world ocean [*Carr*, 2002].

[13] Penetration of UVR in the upper layer increased from MAR to SPG and decreased from SPG to UPW (Table 1). The stations exhibiting the clearest waters were found in the vicinity of Easter Island with STB7 and GYR followed by STB12 and STB5 (Figure 1). The lowest values of $K_d(\lambda)$ at 305, 325, 340 and 380 nm were 0.083, 0.055, 0.039 and 0.021 m^{-1}, respectively (Table 1). These data are in good agreement with those obtained by *Morel et al.* [2007] using the LI-1800 UW spectro-radiometer. The station exhibiting the most turbid waters was UPW followed by STB18 and MAR. For all the stations, $K_d(\lambda)$ decreased from the UV-B to UV-A spectral domain. $K_{d,PAR}$ was lower than K_d(380 nm) only for the most turbid waters (Table 1). The linear correlation between $K_d(\lambda)$ and in situ surface Chl a concentration was very highly significant for 380 nm ($r^2 = 0.72$, $p < 0.001$, $n = 12$) and highly significant for 305, 325, 340 nm and PAR ($r^2 = 0.57–0.66$, $p < 0.01$, $n = 12$). Several studies have shown significant linear correlations between Chl a and UV-A/Blue radiation in very coastal waters or open ocean [*Stambler et al.*, 1997; *Figueroa*, 2002]. Although Chl a does not present high absorption for UV wavelengths, these relationships could be attributed to substances that covary with Chl a such as CDOM, which

is the main contributor to UVR attenuation in natural waters.

[14] Assuming a vertical homogeneity of the distribution of attenuating substances and organisms over the depth interval 0^- m to DCM, $Z_{10\%}(UV)$ were extrapolated from $K_d(UV)$. $Z_{10\%}(UV)$ were considered as representative of the depth interval 0^- m - DCM since they were always located above the DCM. The penetration of UVR found in STB7 was compared with those reported for the clearest natural waters (Figure 2). In STB7, $Z_{10\%}(UV)$ were much higher than those characterizing the (previous) clearest oceanic waters, i.e. Type OI waters in the Jerlov system of classification [*Jerlov*, 1976; *Smith and Baker*, 1981] and the Subtropical Atlantic Ocean [*Obernosterer et al.*, 2001]. Thus, we measured in the hyper-oligotrophic waters of the SPG (STB4, STB5, STB7, GYR and STB12) the highest UVR penetration ever reported for the marine environment. These highly UVR-transparent waters represent an oceanic area of great magnitude: about 3000 km along the transect (Figure 1). Interestingly, $Z_{10\%}(UV)$ in STB7 were similar to those of the purest fresh waters, i.e. Venda Lake [*Vincent et al.*, 1998] and Crater Lake [*Hargreaves et al.*, 2007] (Figure 2).

[15] When the UV-extended IOP model was used assuming the Case 1 water model with S = 0.017 nm^{-1} over the UV spectral domain, we observed a significant agreement between measured and computed $K_d(\lambda)$ for UV-A (325, 340, 380 nm). However, for UV-B (305 nm), we found large underestimations that increased from the clearest (29%) to the most turbid (49%) waters (Figure 3a). This IOP model was validated in the North Pacific by *Vasilkov et al.* [2005]. The latter found better linear correlations between measured and computed $K_d(\lambda)$, i.e. $r^2 = 0.79$ for 313, 320 and 340 nm, and 0.76 for 380 nm, but with the relative standard deviation between measured and computed values of about 20% for all the stations, which is close to that observed with our data in the UV-A range. It is important to notice that this is the first time that such comparisons are conducted for 305 nm, which is a strongly CDOM-dependent wavelength, leading to higher discrepancies compared to longer UV wavelengths. In order to get a better estimation of computed $K_d(\lambda)$ at 305 nm, we performed a sensitivity study on the S value. Indeed, two other extrapolations were made from $a_{CDOM}(440)$ with higher S values, i.e. 0.020 and 0.023 nm^{-1}. The better agreement was observed when combining two separate one-S-value extrapolations, i.e. S = 0.017 nm^{-1} at 325, 340, 380 nm and S = 0.023 nm^{-1} at 305 nm (Figure 3b). In the same way, *Morel et al.* [2007] employed an inverse model to recover S values over the UV spectral domain. They found S = 0.0164 nm^{-1} for 370–400 nm and S = 0.019 to 0.027 nm^{-1} for 310–370 nm. Consequently, in the south east Pacific waters, there is probably not continuity in CDOM absorption spectral slope coefficient in the UV domain but steeper slope coefficients.

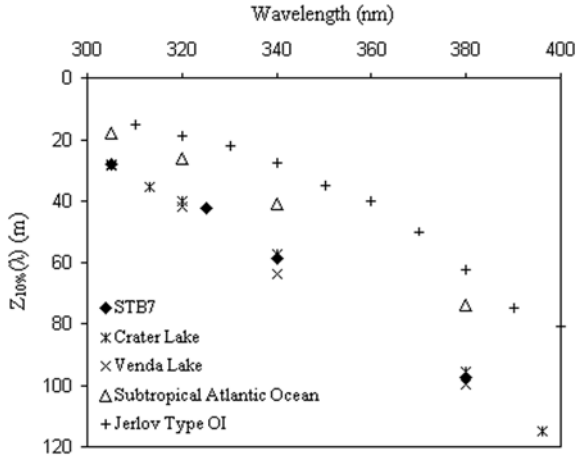

Figure 2. $Z_{10\%}(\lambda)$ at 305 nm (UV-B), and 325, 340 and 380 nm (UV-A) determined between 0^- and 30 m in the hyper-oligotrophe zone of the South Pacific Gyre (STB7 station). For comparison, we reported $Z_{10\%}(UV)$ values obtained for the clearest oceanic waters, i.e. the Jerlov Type OI waters [*Jerlov*, 1976; *Smith and Baker*, 1981] and the Subtropical Atlantic Ocean (23°N, 38°W) [*Obernosterer et al.*, 2001], and for the clearest fresh waters, i.e. the Crater Lake (Oregon) [*Hargreaves et al.*, 2007] and the Venda Lake (Antarctic) [*Vincent et al.*, 1998].

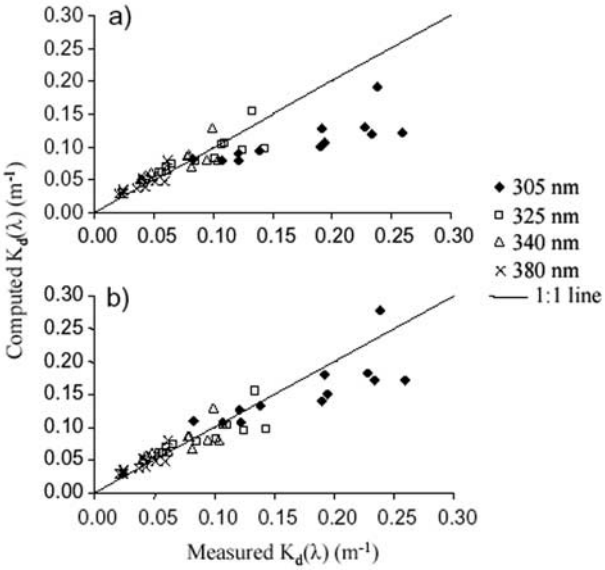

Figure 3. Comparison between measured and computed $K_d(\lambda)$ at 305 nm (UV-B), and 325, 340 and 380 nm (UV-A) between 0^- and 15 or 30 m for the stations of the south east Pacific, except UPW (n = 12). Measured $K_d(\lambda)$ were derived from in situ optical measurements whereas computed $K_d(\lambda)$ were calculated from UV-extended IOP and RT models. The UV-extended IOP model was used with in situ surface Chl a concentration (see Table 1) as input parameter assuming the Case 1 water model. Different values of CDOM absorption spectral slope coefficient (S) were used: (a) S = 0.017 nm^{-1} over the UV spectral domain (at 305, 325, 340 and 380 nm) as proposed by *Kopelevich et al.* [1989] and used by *Vasilkov et al.* [2005] in the North Pacific waters and (b) S = 0.017 nm^{-1} at 325, 340, 380 nm and S = 0.023 nm^{-1} at 305 nm, combined from two separate one-S-value extrapolations. For Figures 3a and 3b, the determination coefficient (r^2) of the linear correlation was 0.60, $p < 0.01$ at 305 nm, 0.67, $p < 0.01$ at 325 nm, 0.65, $p < 0.01$ at 340 nm and 0.76, $p < 0.001$ at 380 nm.

[16] **Acknowledgments.** We are grateful to the captain and crew of the RV "*Atalante*" for excellent service during the BIOSOPE cruise. We acknowledge the chiefs scientist of the cruise, i.e. H. Claustre and A. Sciandra. We also thank M. Chami for his helpful comments as well as the two anonymous reviewers for improving the quality of the manuscript. This research was funded by CNRS-PROOF projects BIOSOPE and UVECO, and the region of Provence Alpes Côte d'Azur.

References

Andrié, C., I. Bouloubassi, H. Cornu, R. Fichez, C. Perre, and F. Rougerie (1992), Chemical and tracer studies in coral reef interstitial waters (French Polynesia): Implications for endo-upwelling circulation, paper presented at 7th International Coral Reef Symposium, Univ. of Guam, Guam.

Buma, A. G. J., P. Boelen, and W. H. Jeffrey (2003), UVR-induced DNA damage in aquatic organisms, in *UV Effects in Aquatic Organisms and Ecosystems*, edited by E. W. Helbling and H. E. Zagarese, pp. 291–327, Eur. Soc. for Photobiol., Pisa, Italy.

Carr, M. E. (2002), Estimation of potential productivity in Eastern Boundary currents using remote sensing, *Deep Sea Res., Part II*, *49*, 59–80.

Claustre, H., and S. Maritorena (2003), The many shades of ocean blue, *Science*, *302*, 1514–1515.

Figueroa, F. L. (2002), Bio-optical characteristics of Gerlache and Bransfield Strait waters during an Antarctic summer cruise, *Deep Sea Res., Part II*, *49*, 675–691.

Fougnié, B., P. Henry, A. Morel, D. Antoine, and F. Montagner (2002), Identification and characterization of stable homogeneous oceanic zones: Climatology and impact on in-flight calibration of space sensor over Rayleigh scattering, in *Ocean Optics XVI* [CD-ROM], Off. of Nav. Res., Santa Fe, N. M.

Fry, E. S. (2000), Visible and near ultraviolet absorption spectrum of liquid water, *Appl. Opt.*, *39*, 2743–2744.

Gordon, H., O. Brown, R. Evans, J. Brown, R. Smith, K. Baker, and D. Clark (1988), A semi-analytical radiance model of ocean color, *J. Geophys. Res.*, *93*, 10,909–10,924.

Hargreaves, B. R., S. F. Girdner, M. W. Buktenica, R. W. Collier, E. Urbach, and G. L. Larson (2007), Ultraviolet radiation and bio-optics in Crater Lake, Oregon, *Hydrobiology*, *574*, 107–140.

Herbland, A., A. Lebouteiller, and P. Raimbault (1985), Size structure of phytoplankton biomass in the equatorial Atlantic Ocean, *Deep Sea Res.*, *32*, 819–836.

Jerlov, N. G. (1976), *Marine Optics*, Elsevier, New York.

Kopelevich, O. V., S. V. Lutsarev, and V. V. Rodionov (1989), Light spectral absorption by yellow substance of ocean water, *Oceanology*, *29*, 409–414.

Mobley, C. D. (1994), *Light and Water: Radiative Transfer in Natural Waters*, Academic Press, San Diego, Calif.

Mopper, K. and D. J. Kieber (2002), Photochemistry and the cycling of carbon, sulphur, nitrogen and phosphorus, in *Biogeochemistry of Marine Dissolved Organic Matter*, edited by D. A. Hansell and C. A. Carlson, pp. 455–507, Academic Press, San Diego, Calif.

Morel, A. (1988), Optical modelling of the upper ocean in relation to its biogenous matter content (Case I waters), *J. Geophys. Res.*, *93*, 10,749–10,768.

Morel, A., and S. Maritorena (2001), Bio-optical properties of oceanic waters: A reappraisal, *J. Geophys. Res.*, *106*, 7163–7180.

Morel, A., B. Gentili, H. Claustre, M. Babin, A. Bricaud, J. Ras, and F. Tieche (2007), Optical properties of the "clearest" natural waters, *Limnol. Oceanogr.*, *52*, 217–229.

Obernosterer, I., P. Ruardij, and G. J. Herndl (2001), Spatial and diurnal dynamics of dissolved organic matter (DOM) fluorescence and H_2O_2 and the photochemical oxygen demand of surface water DOM across the subtropical Atlantic Ocean, *Limnol. Oceanogr.*, *46*, 632–643.

Raimbault, P., G. Slawyk, B. Boudjellal, C. Coatanoan, P. Conan, B. Coste, N. Garcia, T. Moutin, and M. Pujo-Pay (1999), Biomass, new production and export in the equatorial Pacific at 150°W: Evidence for intense nitrogen recycling, *J. Geophys. Res.*, *104*, 3341–3356.

Signorini, S. R., C. R. McClain, and Y. Dandonneau (1999), Mixing and phytoplankton bloom in the wake of the Marquesas Islands, *Geophys. Res. Lett.*, *26*, 3121–3124.

Smith, R. C., and K. S. Baker (1981), Optical properties of the clearest natural waters (200–800 nm), *Appl. Opt.*, *20*, 177–184.

Smith, R. C., and K. S. Baker (1984), Analysis of ocean optical data, *Proc. SPIE Soc. Opt. Eng.*, *478*, 119–126.

Stambler, N., C. Lovengreen, and M. M. Tilzer (1997), The underwater light field in the Bellingshausen and Amundsen Seas (Antarctica), *Hydrobiology*, *344*, 41–56.

Tedetti, M., and R. Sempéré (2006), Penetration of ultraviolet radiation in the marine environment: A review, *Photochem. Photobiol.*, *82*, 389–397.

Vasilkov, A., N. Krotkov, J. Herman, C. McClain, K. Arrigo, and W. Robinson (2001), Global mapping of underwater UV irradiances and DNA-weighted exposures using Total Ozone Mapping Spectrometer and Sea-viewing Wide Field-of-view Sensor data products, *J. Geophys. Res.*, *106*, 27,205–27,219.

Vasilkov, A. P., J. R. Herman, Z. Ahmad, M. Kahru, and B. G. Mitchell (2005), Assessment of the ultraviolet radiation field in ocean waters from space-based measurements and full radiative transfer calculations, *Appl. Opt.*, *44*, 2863–2869.

Vincent, W. F., R. Rae, I. Laurion, C. Howard-Williams, and J. C. Priscu (1998), Transparency of Antarctic ice-covered lakes to solar UV radiation, *Limnol. Oceanogr.*, *43*, 618–624.

Whitehead, R. F., S. J. de Mora, and S. Demers (2000), Enhanced UV radiation—A new problem for the marine environment, in *The Effects of UV Radiation in the Marine Environment*, edited by S. de Mora, S. Demers, and M. Vernet, pp. 1–34, Cambridge Univ. Press, London.

B. Charrière, D. Nérini, R. Sempéré, and M. Tedetti, Laboratoire de Microbiologie Géochimie et Ecologie Marines (LMGEM), UMR 6117, Centre d'Océanologie de Marseille, Université de la Méditerranée, Campus de Luminy, Case 901, F-13288 Marseille Cedex 9, France. (richard.sempere@univmed.fr)

K. Kawamura, Institute of Low Temperature Science, Hokkaido University, N19 W8, Kita-ku, Sapporo 060-0819, Japan.

W. L. Miller, Department of Marine Sciences, University of Georgia, Athens, GA 30602-3636, USA.

P. Raimbault, Laboratoire d'Océanographie et de Biogéochimie, UMR 6535, Centre d'Océanologie de Marseille, Université de la Méditerranée, Campus de Luminy, Case 901, F-13288 Marseille Cedex 9, France.

M. A. Vasilkov, Science Systems and Applications, Inc., 10210 Greenbelt Road, Lanham, MD, USA.